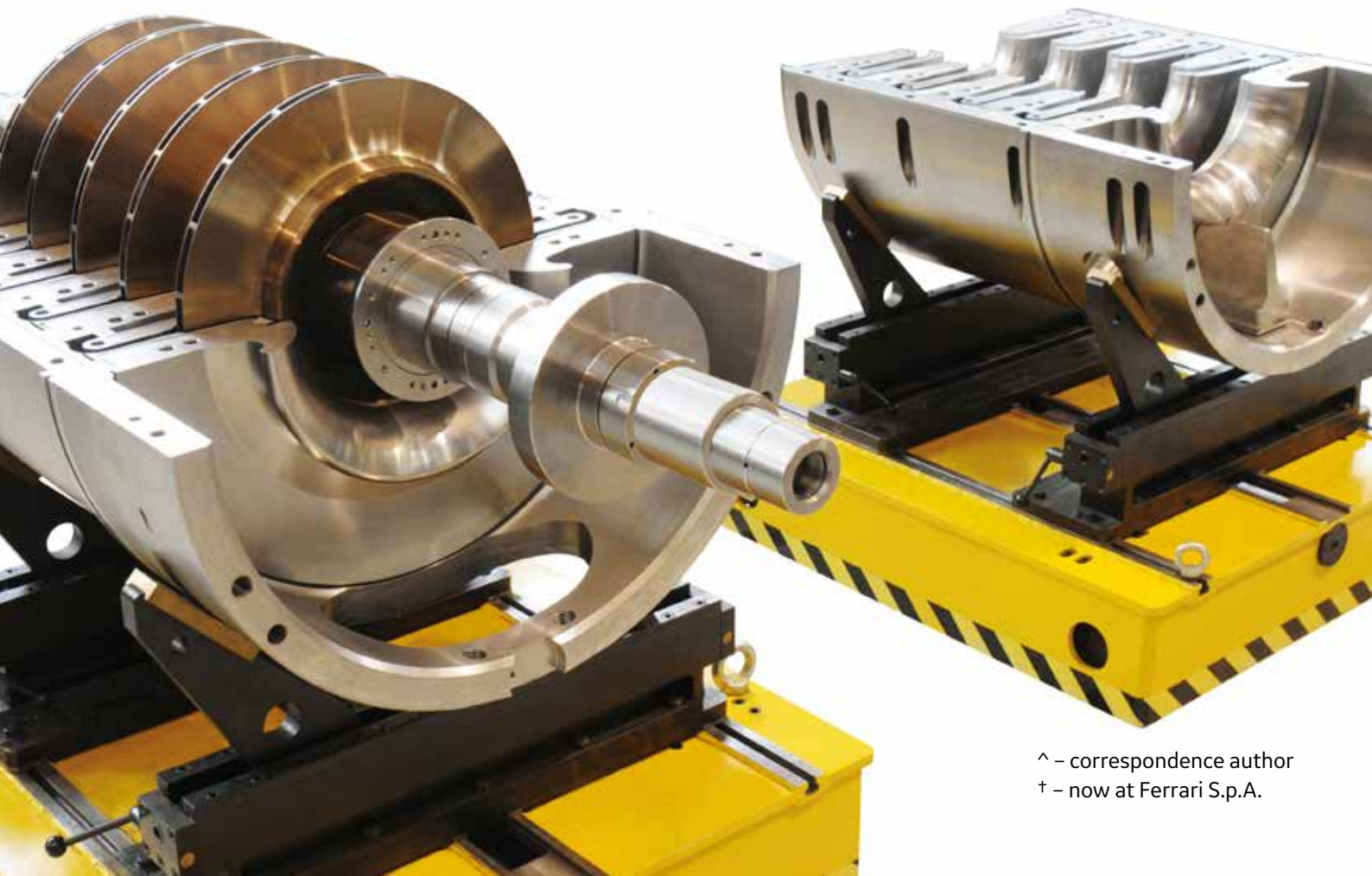


DOWNSTREAM TECHNOLOGY SOLUTIONS | PRODUCTS & SERVICES

# Centrifugal compressors return channel optimization by means of advanced 3-D computational fluid dynamics



<sup>^</sup> – correspondence author  
<sup>†</sup> – now at Ferrari S.p.A.

## Abstract

In the oil and gas industry, the quest for high efficiency turbomachinery continuously drives technological advancement. While rotor (impeller) enhancements are a common practice related to the design of centrifugal compressors – seen both in scientific literature and in actual industrial experience – the same focus is not always applied to improving statoric components. This is because plenums and return channels make a smaller impact on overall compressor performance compared to the impeller. However, addressing losses related to statoric parts can significantly improve the design of the centrifugal compressors stage, especially considering the advanced level of aerodynamic detail that has been reached by original equipment manufacturers (OEMs).

GE has enhanced the return channel using 3-D computational fluid dynamics (CFD) to significantly reduce the loss coefficient. The CFD simulations were run with TACOMA, GE's non-commercial, proprietary software, and steady flow was computed with Reynolds Averaged Navier Stokes (RANS) approach and turbulence  $\kappa$ - $\omega$  model with strain correction. A full validation of the employed method was performed previously against experimental campaigns and is available in the referenced literature.

To closely reproduce full-stage operating conditions, simulations ideally should include impeller, diffuser and return channel. Unfortunately, the computational cost of a multi-iteration optimization was not feasible. To preserve simulation accuracy while reducing the domain, flow profiles at the impeller exit were imposed at the considered computational domain inlet (the diffuser inlet), while cavity effects and secondary flows were accounted for by adding source terms taken from the full-stage simulation of the baseline geometry.

Return channel blades were parameterized in terms of angle distributions with Bézier curves at the hub and shroud, for a total of 18 Bézier poles. Each different design was simulated with its speedline consisting of seven operating conditions, whereas progressive optimization based on response surfaces were considered starting from an initial design of experiment (DOE). Of the more than 100 designs simulated, the most efficient allows a 20 percent loss coefficient reduction compared to a real case stage design at design point.

## Nomenclature

$C_p$	static pressure recovery coefficient
$D$	diameter
DOE	design of experiments
DP	design point
GA	genetic algorithm
L3	left (surge) speedline limit
LE	leading edge
$M_u$	peripheral Mach number
$\dot{m}$	mass flow rate
$p$	static pressure
R3	right (choke) speedline limit
$R$	gas constant
RC	return channel
$T$	temperature
$U$	peripheral velocity
$y^+$	dimensionless wall distance

### greek

$\varepsilon$	turbulent dissipation
$\gamma$	ratio of specific heats
$\varphi$	flow coefficient
$\xi$	total pressure loss coefficient
$\omega$	specific dissipation rate
$\eta_p$	polytropic efficiency
$\rho$	density
$\tau$	work coefficient

### subscript

$T$	total quantities
$s$	static quantities
1	impeller inlet
2	impeller outlet/diffuser inlet
3	diffuser outlet/U-bend inlet
4	return channel outlet

# Introduction

Computational fluid dynamics (CFD) has become an important tool for design and performance prediction of centrifugal compressors. In general, steady CFD computations are used during aerodynamic design because they can be performed relatively quickly and provide good overall accuracy. In addition, steady CFD simulations are used extensively to compare the performance of different designs and for design enhancement. Increasing demand for higher centrifugal compressor stage efficiency, wider operating range capability and enhanced machine compactness point to the importance of improving the overall performance prediction capability of the numerical tools while allowing fast design iterations for cost efficiency.

One of the weakest points in CFD calculations is the assessment of stationary components such as the centrifugal compressor U-bend and return channel. Because market demands require stages with high efficiencies and wide operating ranges, the detailed design of stationary components can no longer be considered as a secondary concern.

In the last few years, increased numerical resources and improved modeling tool accuracy have allowed aero-designers to study the flow field inside the cavities of centrifugal compressor stages. Guidotti et al. [1-4] showed that by including leakage flows in the computational domain and using advanced numerical models like curvature corrections, the flow profiles inside stationary components are correctly detached and a strong agreement with test data can be reached. Figure 1 assesses the impact of neglecting cavities modeling, and highlights a remarkable 3 to 6 percent efficiency shift, as reported in [4].

These studies highlight that the flow through the front and backside cavities of closed impellers greatly influences the overall centrifugal compressor stage performance. Better understanding of the impact of cavity leakage flows on stage performance allows engineers to improve stage design.

Some past works about return channel optimization include Veress and Van den Braembussche [5], who employed an inverse design analytical procedure with prescribed load distribution to obtain a 3-D return channel vane with the leading edge located upstream of the U-bend at the diffuser outlet. This type of downstream-extended return channel is often referred to as “cross-over.” The study’s results, including standard CFD computations, showed a substantial improvement against baseline 2-D channel in terms of increased pressure recovery coefficient and softened secondary flows. However, only a single design point case (not including operating range) was considered, and cavities were not modelled.

Recently, Hildebrandt presented a full 2-D [6] and 3-D [7] optimization with OpenFoam CFD solver and genetic algorithms to significantly reduce the pressure loss coefficient. In his detailed analyses, Hildebrandt obtained interesting improvements in loss reduction without considering cross-over, but again cavities were excluded from the simulation, and it was for design point only.

More recently, Nishida et al. [8] optimized and tested a 2-D return channel with a Latin hypercube sampling initial design of experiments (DOE) followed by a multi-objective genetic algorithms optimization based on Kriging response surfaces.

In their work, the authors parameterized the geometry, varying return channel length, width, angles and blades number, while keeping fixed the U-bend (without cross-over) and leading edge position.

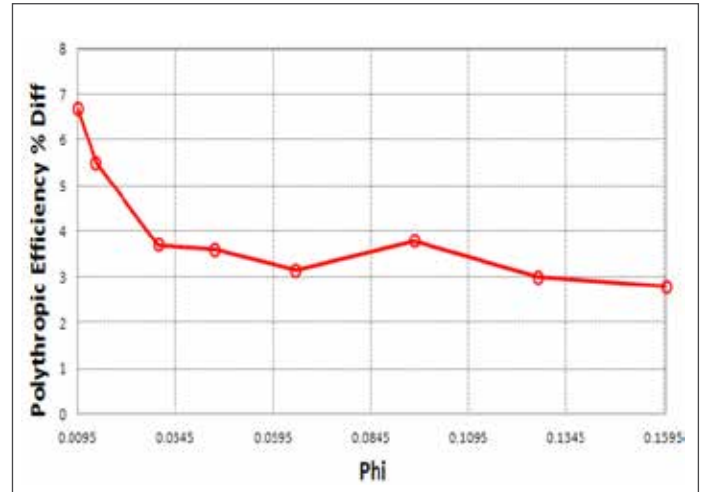


**Figure 1** – Leakage modeling effect: polythropic efficiency difference from the standard case (without cavities) to the case with cavities added to the domain, as reported in [4].

Stage efficiency was shown to increase due to reduced losses (verified during tests), but without a leakage flows assessment.

Moving beyond the previous studies, this study dealt with the enhancement of a cross-over return channel, including cavity effects. An initial and extensive DOE was used to train a response surface. It employed a seven-operating-points speedline for each design. The research team identified an improved design by running an optimization on the DOE-based response surface. Finally, the enhanced design was simulated and compared against the standard baseline case (no cross-over).

The next section describes the approach and numerical models in detail, followed by the problem parameterization. Finally, the initial and final design results are qualitatively and quantitatively compared.

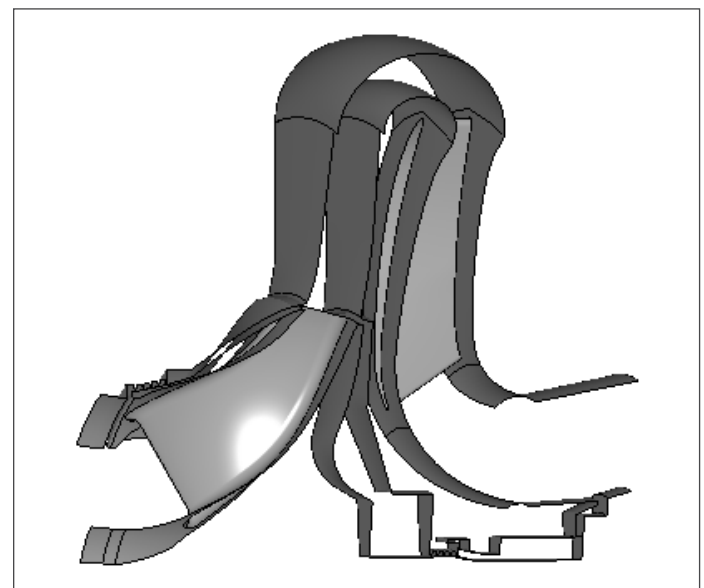


**Figure 2** - Baseline computational fluid domain with fully modeled leakage flows in both hub and shroud cavities

# Methodology and Numerical Models

## Leakage Flows Modeling

As previously discussed, improved stage performance prediction can be achieved by the inclusion of hub and shroud cavities simulation. Nevertheless, leakage flow modeling represents an increase in computational size and time requirements that is not yet affordable for intensive optimization efforts.

To correctly model the flow field inside the stage without increasing user and/or computational time, a two-step simulation approach was employed. Initially, the baseline stage with the entire leakage flow system was simulated (the full computational model including hub and shroud cavity is represented in Figure 2). To obtain the complete speedline, the “full” simulation was repeated for the seven operating points. For each operating point, diffuser inlet profiles were extracted together with the leakage flow conditions after the return channel trailing edge (note that the shroud cavity also affects the diffuser inlet profile).

Finally, both diffuser profiles and leakage flows were used, respectively, as inlet boundary conditions and source terms in the computations during the optimization phase. The underlying assumption in this approach is to consider return channel blade geometry differences from baseline with a second-order effect on leakage flows.

This two-step approach allowed for a massive reduction of the computational effort, but still considered the impact of cavities on the 3-D flow field. Figure 3 shows a schematic of the considered fluid domain with only the diffuser, U-bend, and return channel included.

## Numerical Setup

Simulations were carried out using the GE in-house CFD code TACOMA. TACOMA (**T**urbine **A**nd **C**OMPressor **A**nalysis) is a GE proprietary code used for computational fluid dynamics simulations on axial and radial turbomachinery. TACOMA is a 3-D multi-block, multigrid, structured, non-linear and linear Euler/Navier-Stokes solver for turbomachinery blade rows. TACOMA is a cell-centered explicit flow solver based on the JST scheme [9]. Details of the scheme, as well as validation cases, can be found in [10] and [11]. The solution was obtained via a multi-step Runge-Kutta explicit time marching scheme with convergence acceleration via local time steps, residual averaging, and V-cycle or W-cycle multigrid. In this analysis, steady 3-D Reynolds-Averaged Navier-Stokes (RANS) equations were solved coupled with the two-equation k- $\omega$  turbulence model developed by Wilcox [12]. TACOMA uses the Kato and Launder production modification instead of the original one from the Wilcox model [13].

TACOMA also incorporates a curvature correction model found to be useful on centrifugal compressor stage analysis, as shown by Smirnov et al [14].

Previous validations and modeling experiences with TACOMA on centrifugal compressor stages can be found in [15-19], [1], [2] and [4]. The computational domain includes diffuser and return channel.

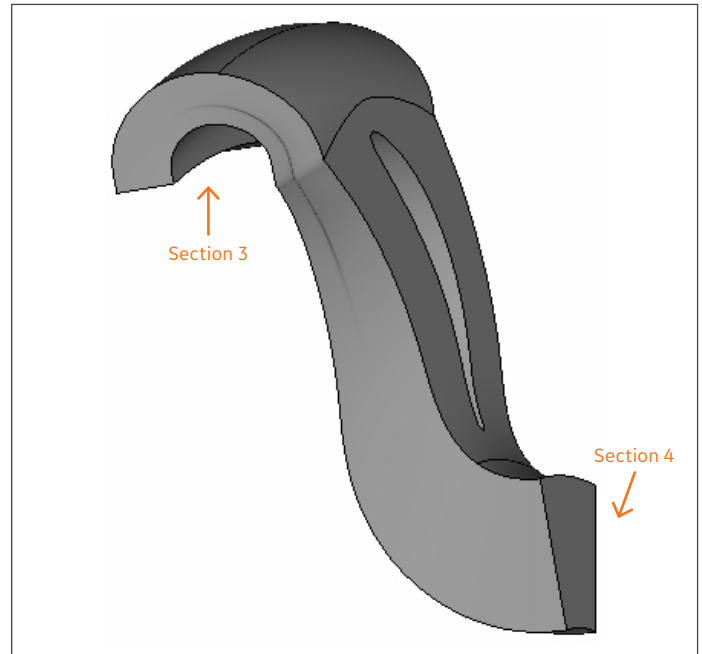


Figure 3 – Baseline RC geometry with section definition

Numerical runs were performed on a single blade sector with periodic boundary conditions, as shown in Figure 4 for one of the test cases.

Diffuser and return channel domain were treated in the stationary reference of frame. Ideal gas properties were specified in all cases.

## Computational Grid

Commercial Numeca Autogrid software was used to generate structured grids for the U-bend and return channel. More details about grid generation and quality can be found in the work already mentioned [1-4]. Wall integration was used to capture the boundary layer, and computational grids were modeled with an average  $y^+$  less than 1 on all the wall surfaces to help ensure good resolution of the viscous sub-layer (see Figure 4). A suction slot was modeled at the end of the return channel to mimic the effect of leakage flow by using a source term (as shown in Figure 5).

## Boundary Conditions and Solver Convergence

As described earlier, flow profiles at the inlet of the computational domain were taken from previous full domain CFD computations, including cavities. In particular, tangential averaged profiles of total quantities and angles were used at the domain inlet. Total pressure, total temperature, and flow angle profiles were applied as inlet conditions. Mass flow rate conditions were applied at the outlet at the different operating conditions. All the walls were modeled as no-slip and adiabatic. Mathematical and physical convergences were constantly monitored during computations.

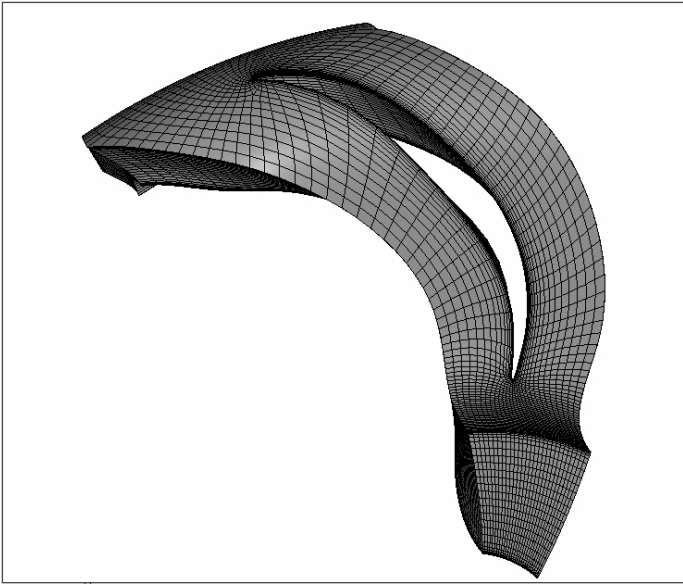


Figure 4 – Computational grid

## Test Case Description

The test case was a centrifugal compressor 3-D impeller stage at high flow coefficient and high peripheral Mach number. The impeller external diameter  $D_2$  was 390 mm. The flow coefficient and peripheral Mach number were defined as in equations (1) and (2) respectively,

$$\varphi = \frac{4Q_{1T}}{\pi D_2^2 U_2} \quad (1)$$

$$Mu = \frac{U_2}{\sqrt{\gamma R T_{1T}}} \quad (2)$$

where  $Q_{1T}$  is the volumetric flow rate (calculated using total density) at impeller inlet. The flow coefficient of the selected stage was 0.1700 and the peripheral Mach number was 1.0.

## Geometry Parameterization

The first step of any optimization is parameter definition. While the parameterization of a statoric, straight 2-D blade might be simple, 3-D blade parameterization is much more complex. The study independently varied only the hub and shroud profiles and constructed the blade by linearly connecting the two. Each profile was defined by angle and thickness distributions in the meridional plane, from leading edge to trailing edge. Angle distributions were parameterized by nine Bézier poles each, for a total of 18 poles, whereas thickness distribution was kept frozen, given some mechanical constraints.

The leading edge of the return channel was moved upstream with respect to the baseline and fixed in the U-bend, which also was unchanged during the process; trailing edge location was constant as well. Figure 5 schematically represents the return channel blade under investigation. Figure 6 shows a typical angle distribution taken from one non-optimal design at the hub section. Parameters were free to change in the allowable ranges defined in Table 1. Then, the DOE algorithm selected 100 designs that combined different values of the involved parameters.

Bézier Pole	SHROUD		HUB	
	min	max	min	max
1	67	73	47	53
2	49	55	54	60
3	43	49	55	61
4	38	44	57	63
5	37	43	57	63
6	-3	3	-3	3
7	-3	3	-3	3
8	-3	3	-3	3
9	-4	4	-4	4

Table 1 – Bézier poles allowable ranges

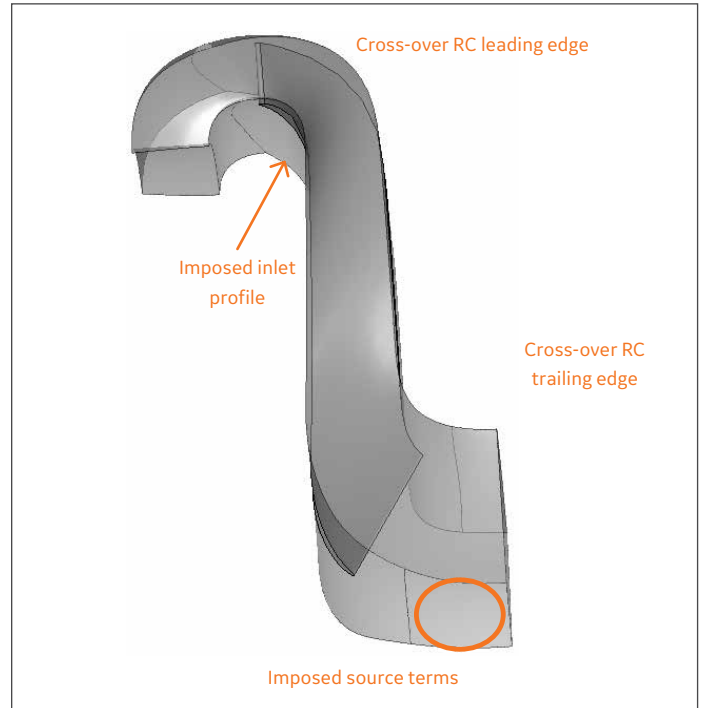


Figure 5 – Return channel geometry with cross-over and mimicked cavities effect

Finally, the new design reduced the number of blades, thus decreasing the solidity; four fewer blades were imposed in the enhancement process with respect to the baseline design.

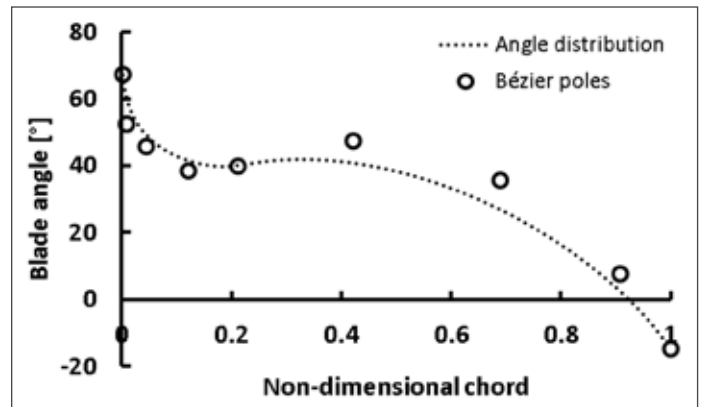


Figure 6 – Example of angle mean line (AML) parameterization for a non-optimal design at hub section

## Results And Discussion

A Latin hypercube algorithm was employed to efficiently explore the design space. The DOE cases were evaluated in terms of total pressure loss coefficient and static pressure recovery coefficient, defined in the following equations (3) and (4):

$$\xi = \frac{P_{4T} - P_{3T}}{P_{3T} - P_{3s}} \quad (3)$$

$$Cp = \frac{P_{4s} - P_{3s}}{P_{3T} - P_{3s}} \quad (4)$$

Once the 100 speedlines were simulated, total pressure loss coefficients at the speedline center (design point) were extracted and a response surface was constructed with the radial basis function (RBF) technique. A genetic algorithm (GA) was then employed to find a significantly improved new design (with reduced losses as the single objective) using the response surface (RS) evaluation method. The three steps composing the optimization (DOE, RS, GA) were performed with the aid of GE's PEZ in-house tool. As a final step, the validation of the enhanced design was carried out by a CFD simulation of the generated case (which was, of course, different from any of the DOE geometries).

The results of the DOE are reported in Figure 7 and expressed in both total pressure loss and static pressure recovery coefficients at design point in a non-dimensional form (by dividing all values with baseline design point original coefficients). The first relevant outcome is that all the geometries performed better than the baseline both in terms of reduced losses (all points less than 85 percent of the baseline) and increased pressure recovery (nearly all points more than 150 percent of the baseline). This is due to the beneficial effect of the cross-over introduction, which is able to improve the return channel efficiency regardless of the imposed angle distribution variations. The enhanced design is also represented coherently with the scope of the work; the genetic algorithm found a design able to significantly reduce losses within the return channel.

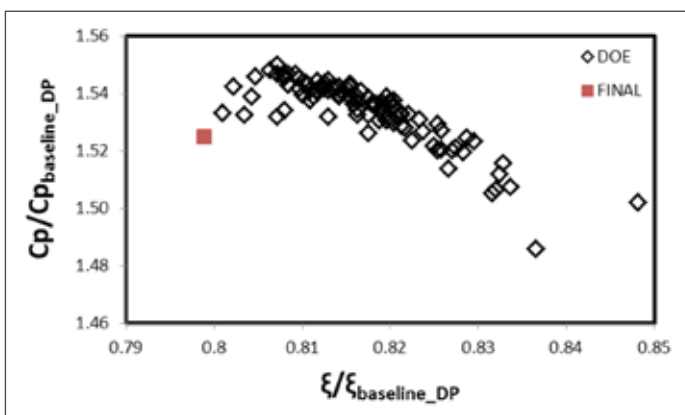


**Figure 7** – DOE and enhanced designs expressed in terms of total pressure loss and pressure recovery coefficient

In addition, the non-optimal performance in terms of pressure recovery was due to single objective optimization rather than multi-objective optimization.

Figure 8 provides an insight of the DOE results in terms of the hub and shroud leading edge angles by graphical interpolation

of 100 discrete points. The non-dimensional total pressure loss coefficient ( $\xi/\xi_{\text{baseline\_DP}}$ ) shows a complex trend overall. The highest losses correspond to angles at both hub and shroud close to the upper bound, due to non-correct flow incidence. From that region of the graph, there is a smooth descending behavior moving toward lower angles, but two relative minimum zones were obtained in two very defined zones. The first was at the lower bound shroud angle and upper hub angle (high lean angle, also the absolute minimum) and the second was at both mild angles. Such a result cannot be considered applicable to any return channel since other Bèzier poles influence performance together with the particular geometry configuration considered in the study. However, it is still worth mentioning that the optimal combination of the parameters can be found even with a DOE approach, often resulting in unpredictable configurations.

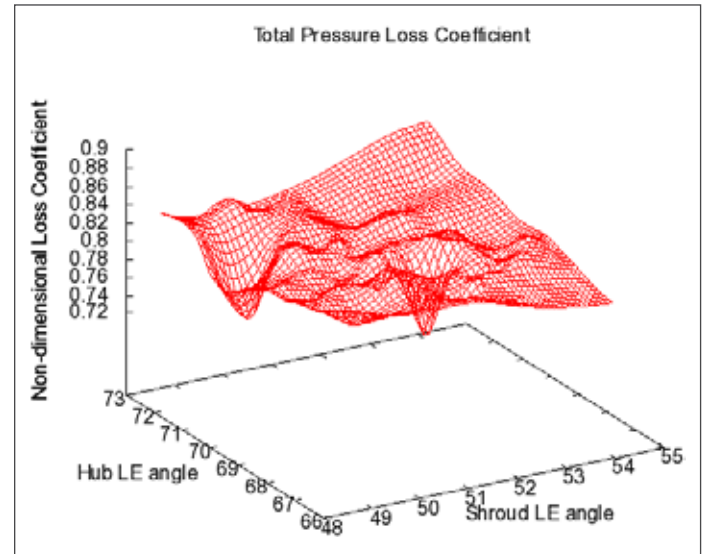


**Figure 8** – Loss coefficient variation as a function of hub and shroud LE edge

To begin to compare the baseline with the improved geometry, loss coefficients were plotted (as shown in Figure 9) for the entire speedline, where "DP" stands for design point and different operating points are numbered with left ("L") and right ("R") notation (so that "L3" is the last operating point before surge and "R3" is the last operating point before complete choke). The enhanced case shows a clear improvement, since all operating points present reduced losses with respect to the baseline (with the exception of the final points at right R2 and R3).

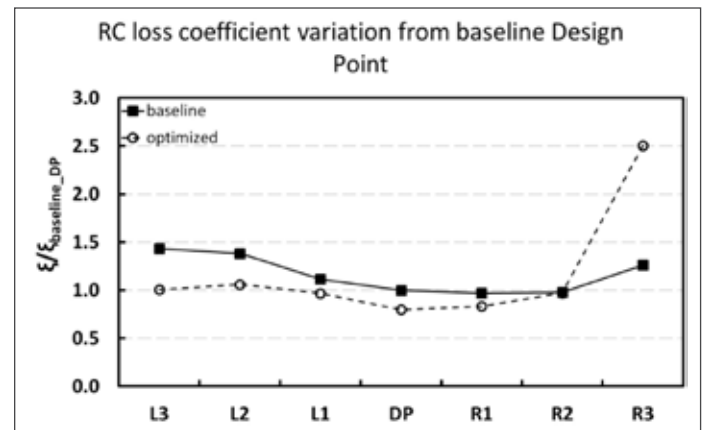


**Figure 9** – Total pressure loss coefficient comparison between baseline and enhanced case (entire speedline)

Such a result was not granted at the beginning of the study, because only the design point was optimized. Again, a multi objective optimization is needed in case of multiple conditions, or at least the addition of some constraints, for example at right and left limit. In this study, the DP was optimized and other points were only verified. The reduced losses have a clear impact on the polytropic efficiency of the whole stage (as shown in Figure 10), again in non-dimensional variation from baseline. Efficiency is enhanced in the entire operating range with the

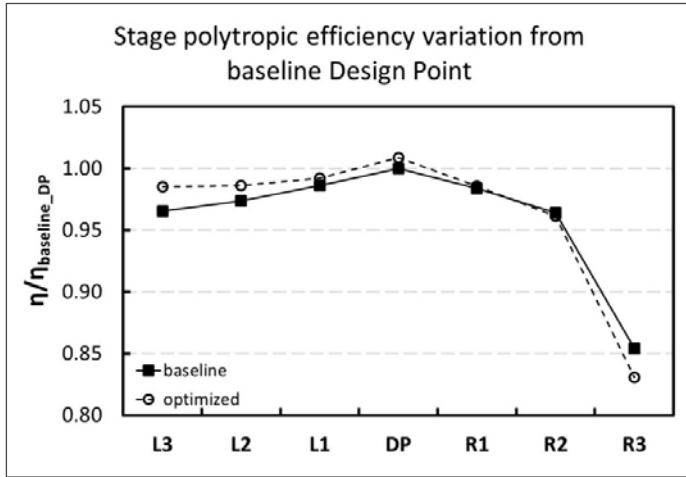


**Figure 10** – Polytropic efficiency comparison between baseline and enhanced case

exception of the right limit; however, the increase at the left limit is more than 4 percent, reducing at nearly 2 percent at design point. Considering that impeller design and flowpath were not included in the optimization, these efficiency increases confirm the value of a stationary components detailed analysis of the return channel in particular. Figure 11 reports pressure recovery coefficient curves that basically show the same trend of loss coefficient but with a smoother trend at right limit. The R2 and R3 operating points are less penalized in terms of  $C_p$  than in  $\xi$  with respect to the baseline. The exit flow angle is considered in Figure 12, showing that the enhanced design always has more positive angles at the return channel outlet.

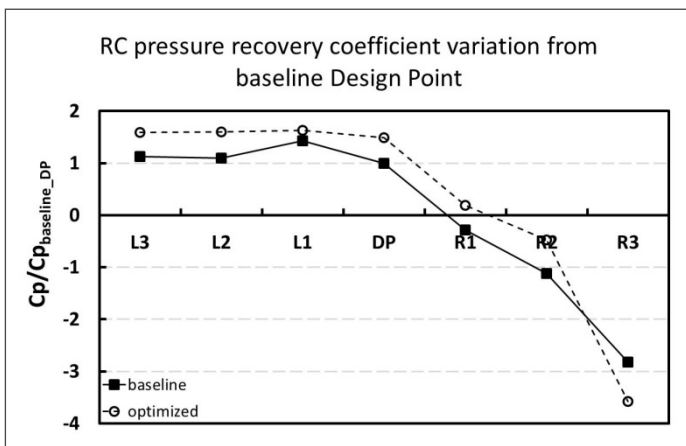


**Figure 11** – Static pressure recovery coefficient comparison between baseline and enhanced case (speedline)

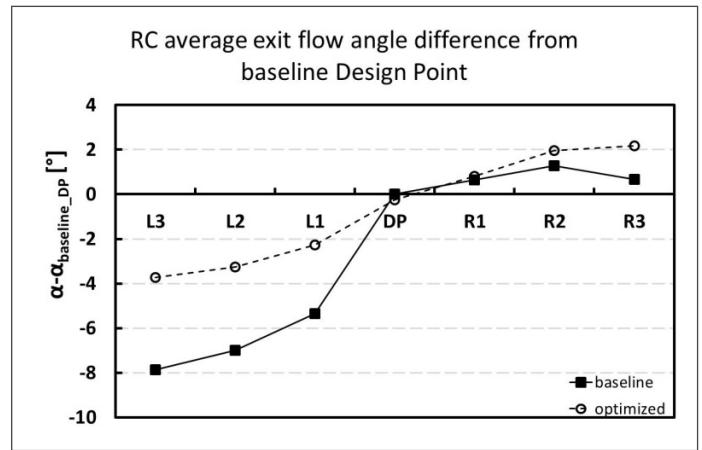


**Figure 12** – Section 4 exit flow angle comparison between baseline and enhanced case

Such behavior reveals that the reduced losses also come from angle optimization in the pre-rotation direction; this has a beneficial effect on the surge limit in multi-stage compressors.

Figures 13 and 14 compare the pressure distributions in terms of static and total pressure, respectively. Additionally, these figures make clear the improvement in terms of higher exit pressure.

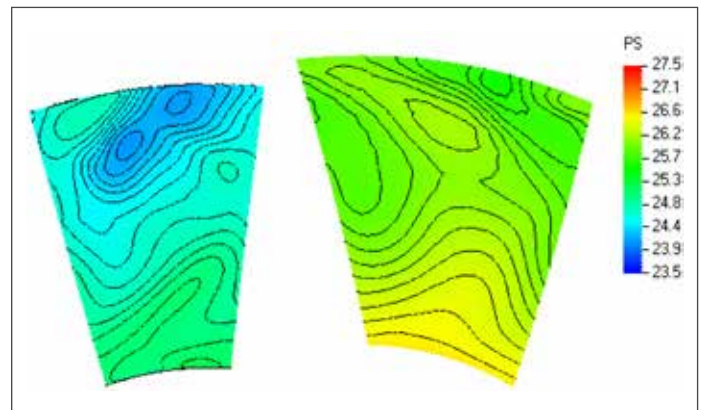


**Figure 13** – Section 4 exit static pressure comparison between baseline (left) and enhanced (right) designs

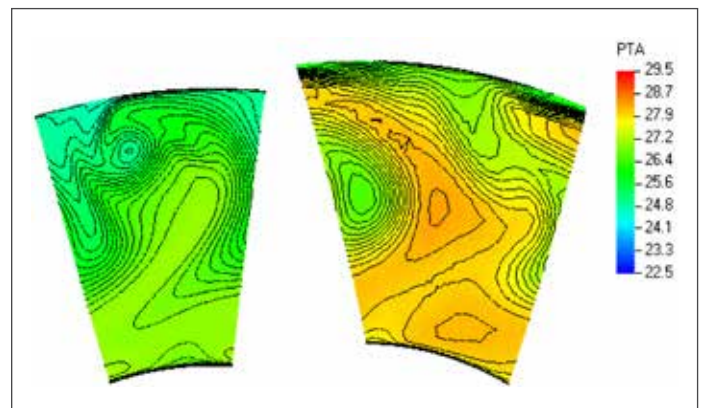


**Figure 14** – Section 4 exit total pressure comparison between baseline (left) and enhanced (right) designs

# Conclusions

GE has optimized a three-dimensional return channel with cross-over, including consideration of the effect of the hub and shroud cavities in the CFD simulation. The entire speedline was considered for each of the 100 cases composing the DOE. Blade angle distribution was varied by means of nine Bézier poles, for a total of 18 parameters, with the objective of total pressure loss coefficient reduction at design point. Some mechanical constraints also were considered in the problem definition, but were not directly included in the study.

A DOE-based response surface was constructed and the final design was obtained by means of a genetic algorithm virtual optimization. The virtual optimum was validated with CFD and revealed a significant improvement of loss coefficient for the whole operating range with the exception of the right limit. In particular, the overall stage polytropic efficiency was improved by 2 percent at design point and nearly 4 percent at left limit due to RC redesign only. The modified RC blade is able to produce a more pre-rotated exit flow angle in particular at left limit, which also provides an enlarged surge limit in the case of a multi-stage compressors arrangement.

Project results confirmed the relevance of the accurate aerodynamic design of centrifugal compressors stationary parts, which traditionally are less refined than impeller blades. Future works will focus on multi-objective optimization with an increased number of parameters, and also will include mechanical constraints.

# References

- 1 Guidotti, E., Tapinassi, L., Naldi, G., and Chockalingam, V., 2012. "Cavity flow modeling in an industrial centrifugal compressor stage at design and off-design conditions". In ASME Turbo Expo 2012. ASME Paper GT2012-68288.
- 2 Guidotti, E., Tapinassi, L., and Naldi, G., 2012. "Influence of seal leakages modeling on low flow coefficient centrifugal compressor stages performance". In ATI Congress 2012, Trieste, Italy.
- 3 Satish, K., Guidotti, E., Rubino, D., Tapinassi, L., and Prasad, S., 2013. "Accuracy of centrifugal compressor stages performance prediction by means of high fidelity cfd and validation using advanced aerodynamic probe". In ASME Turbo Expo 2013. ASME Paper GT2013-95618.
- 4 Guidotti, E., Rubino, D., Tapinassi, L., Naldi, G., Toni, L., Satish, K., and Prasad, S., 2014. "Influence of cavity flows modeling on centrifugal compressor stages performance prediction across different flow coefficient impellers". In ASME Turbo Expo 2014. ASME Paper GT2014-25830.
- 5 Veress, A., Van den Braembussche, R., 2004. "Inverse Design and Optimization of a Return Channel for a Multistage Centrifugal Compressor". Journal of Fluids Engineering, September 2004, Vol. 126, 799-806.
- 6 Hildebrandt, A., 2011. "Aerodynamic Optimisation of a Centrifugal Compressor Return Channel and U-turn with Genetic Algorithms". In ASME Turbo Expo 2011. ASME Paper GT2011-45067.
- 7 Hildebrandt, A., 2012. "Numerical Analysis of Overall Performance and Flow Phenomena of an Automatically Optimized Three-Dimensional Return Channel System for Multistage Centrifugal Compression Systems". In ASME Turbo Expo 2012. ASME Paper GT2012-68559.
- 8 Nishida, Y., Kobayashi, H., Nishida, H., Sugimura, K., 2013. "Performance Improvement of a Return Channel in a Multistage Centrifugal Compressor Using Multiobjective Optimization". Journal of Turbomachinery, May 2013, Vol. 135, 031026 1-8.
- 9 Jameson, A., Schmidt, W., and Turkel, E., 1981. "Numerical solution of the Euler equations by finite volume methods using Runge-Kutta time-stepping schemes". In AIAA 14th Fluid and Plasma Dynamics Conference, Palo Alto, California..
- 10 Holmes, D. G., Mitchell, B. E., and Lorence, C. B., 1997. "Three dimensional linearized Navier-Stokes calculations for flutter and forced response". In ISUATT Symposium.
- 11 Kapetanovic, S. M., N., F. F., G., H. D., and M., O., 2007. "Impact of combustor exit circumferential flow gradients for gas turbine prediction". In In Proceedings of the 5th International Conference on Heat and Mass transfer.
- 12 Wilcox, D. C., 1998. Turbulence Modeling for CFD. DCW Industries, Inc., La Cañada, CA.
- 13 Launder, B. E., M., and Kato, 1993. "Modeling flow induced oscillations in turbulent flow around a square cylinder". In ASME FED, 57, pp 189-199.
- 14 Smirnov, P., and Menter, F., 2008. "Sensitization of the sst turbulence model to rotation and curvature by applying the Spalart-Shur correction term". In ASME Turbo Expo 2008. ASME Paper GT2008-50480.
- 15 Grimaldi, A., Tapinassi, L., Biagi, F. R., Michelassi, V., Bernocchi, A., and Guenard, D., 2007. "Impact of inlet swirl on high-speed high-flow centrifugal stage performance". In ASME Turbo Expo 2007. ASME Paper GT2007-27202.
- 16 Scotti, A. D. G., Biagi, F. R., Sassanelli, G., and Michelassi, V., 2007. "A new slip factor correlation for centrifugal impellers in a wide range of flow coefficients and peripheral Mach numbers". In ASME Turbo Expo 2007. ASME Paper GT2007-27199.
- 17 Aalburg, C., Simpson, A., Schmitz, M. B., Michelassi, V., Evangelisti, S., Belardini, E., and Ballarini, V., 2008. "Design and testing of multistage centrifugal compressors with small diffusion ratios". In ASME Turbo Expo 2008. ASME Paper GT2008-51263.
- 18 Guidotti, E., Tapinassi, L., Toni, L., Bianchi, L., Gaetani, P., and Persico, G., 2011. "Experimental and numerical analysis of the flow field in the impeller of a centrifugal compressor stage at design point". In ASME Turbo Expo 2011. ASME Paper GT2011-45036.
- 19 Ramakrishnan, K., Richards, S., Moyroud, F., and Michelassi, V., 2011. "Multi-blade row interactions in a low pressure ratio centrifugal compressor stage with vaned diffuser". In ASME Turbo Expo 2011. ASME Paper GT2011-45932.



## Imagination at work

### **GE Oil & Gas - Global Headquarters**

The Ark - 201 Talgarth Road, Hammersmith - London, W6 8BJ, UK  
T +44 207 302 6000  
customer.service.center@ge.com

### **Nuovo Pignone S.p.A. - Nuovo Pignone S.r.l**

Via Felice Matteucci, 2 - 50127 Florence, Italy  
T +39 055 423 211  
F +39 055 423 2800

### **Downstream Technology Solutions**

4424 West Sam Houston Parkway North - Houston, TX 77041-8200, US

Centrifugal compressors return channel optimization by means of advanced 3-D computational fluid dynamics

By Fabio De Bellis<sup>^</sup>, Emanuele Guidotti<sup>†</sup>, Dante Tommaso Rubino

© GT 2015-44143 ASME

GEA31968 (07/2015)